Signal Recognition Particle Receptor Exposes the Ribosomal Translocon Binding Site

Mario Halic, *et al.*

Science **312**, 745 (2006);
DOI: 10.1126/science.1124864

Science (print ISSN 0036-8075; online ISSN 1095-9203) is published weekly, except the last week in December, by the American Association for the Advancement of Science, 1200 New York Avenue NW, Washington, DC 20005.

Signal Recognition Particle Receptor Exposes the Ribosomal Translocon Binding Site

Mario Halic,[1]* Marco Gartmann,[1]* Oliver Schlenker,[2] Thorsten Mielke,[3] Martin R. Pool,[4] Irmgard Sinning,[2] Roland Beckmann[1,3]*†

Signal sequences of secretory and membrane proteins are recognized by the signal recognition particle (SRP) as they emerge from the ribosome. This results in their targeting to the membrane by docking with the SRP receptor, which facilitates transfer of the ribosome to the translocon. Here, we present the 8 angstrom cryo–electron microscopy structure of a "docking complex" consisting of a SRP-bound 80*S* ribosome and the SRP receptor. Interaction of the SRP receptor with both SRP and the ribosome rearranged the S domain of SRP such that a ribosomal binding site for the translocon, the L23e/L35 site, became exposed, whereas Alu domain–mediated elongation arrest persisted.

Most secretory or membrane proteins carry N-terminal signal sequences that bind to the SRP, a conserved ribonucleoprotein complex (*1*). After binding SRP, the resulting complex is targeted in a guanine nucleotide triphosphate (GTP)–dependent manner to the plasma membrane in bacteria or the endoplasmic reticulum in eukaryotes via the SRP receptor (SR). This GTP-dependent docking reaction coordinates the presence of a signal sequence on the ribosome with the presence of a vacant translocon (*2*). The transfer of the ribosome nascent chain complex (RNC) from SRP to the translocon occurs before GTP hydrolysis (*3*, *4*). A direct interaction between SR and the translocon has been demonstrated in prokaryotic cells (*5*), and an interaction between SR and the ribosome is suggested in eukaryotic (*6*) and prokaryotic cells (*7*).

In eukaryotes, SR is a heterodimeric complex formed by two GTPase subunits, SRα (FtsY in *Escherichia coli*) and the integral membrane protein SRβ. SRα consists of an N-terminal X domain, which interacts with SRβ (X1), and, connected by a positively charged linker region (X2), a conserved GTP-binding NG domain (*8*), which is homologous to the NG domain of SRP54 (Ffh in *E. coli*).

The SRP-SR interaction involves primarily the NG domains of SRP54 and SRα. A prerequisite for stable complex formation is GTP binding by both NG domains interacting in a twinlike conformation (*9*, *10*). Both NG domains act as mutual GTPase-activating proteins (GAPs) (*11*), and GTP hydrolysis leads to dissociation (*3*).

Crystal structures of the SRαX1-SRβ complex (*8*, *12*) show GTP present in the active site, suggesting catalytic inactivity of SRβ in complex with SRα. The interaction between SRαX and SRβ is GTP dependent, and GTP hydrolysis would result in dissociation (*8*).

It is not known how SR interacts with SRP in the context of the SRP-RNC targeting complex. The targeting complex itself is unable to interact directly with the translocon (*13*) due to overlapping binding sites of SRP (*14*) and translocon at the ribosomal tunnel exit (*15*). The presence of SR, however, allows translocon binding (*13*) and leads to structural rearrangements of SRP, which suggests a distinct mode of ribosome binding (*16*). The question thus remains: How does SR prime the SRP-RNC targeting complex to allow the transfer of the signal sequence and RNC to the translocon?

The SR-SRP-RNC complex was reconstituted in vitro (*14*, *17*). Stalled RNCs were used for the reconstitution with excess amounts of purified mammalian SRP and recombinant SR [lacking the transmembrane domain of SRβ (*18*)]. Sucrose density gradient centrifugation confirmed

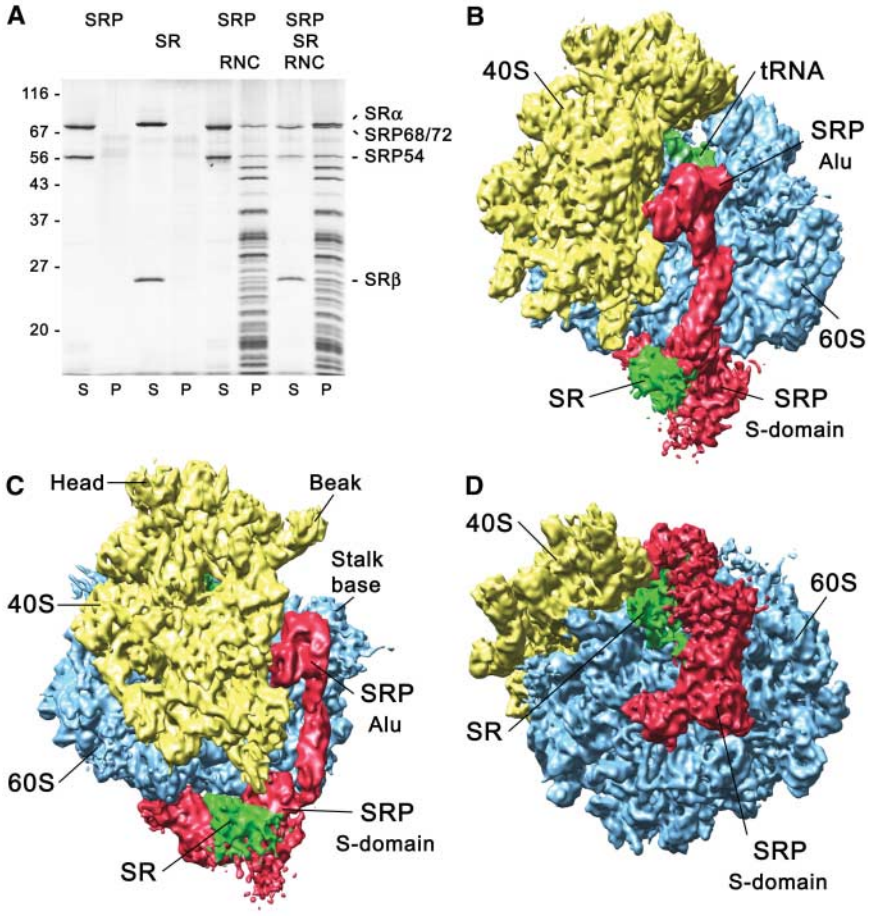

Fig. 1. Reconstitution and cryo-EM structure of the 80*S* ribosome-SRP-SR docking complex. (**A**) Binding assay using purified RNCs (RNC) with an excess of purified SRP and SR in the presence of GMP-PNP. Supernatant (S) and pellet (P) fractions were analyzed by SDS–polyacrylamide gel electrophoresis and Coomassie blue staining. SRP and SR bind stably to RNCs, and both subunits of SR, SRα and SRβ, are detectable in the bound fraction. (**B**) Cryo-EM reconstruction of the 80*S* RNC-SRP-SR complex. The 40*S* small ribosomal subunit is shown in yellow, 60*S* large subunit is in blue, P-site tRNA is in green, and SRP is in red. Additional density at the S domain of SRP is shown in bright green. Landmark features are indicated. (**C**) Same as (B), rotated by 45° around the central vertical axis. (**D**) Same as (B), rotated by 90° backward around a central horizontal axis.

[1]Institute of Biochemistry, Charité, University Medical School Berlin, Monbijoustrasse 2, 10117 Berlin, Germany. [2]Heidelberg University Biochemistry Center (BZH), Im Neuenheimer Feld 328, D-69120 Heidelberg, Germany. [3]UltraStructureNetwork, USN, Max Planck Institute for Molecular Genetics, Ihnestrasse 63-73, 14195 Berlin, Germany. [4]University of Manchester, Faculty of Life Sciences, Michael Smith Building, Oxford Road, Manchester M13 9PT, UK.

*Present address: Gene Center, University of Munich, Department of Chemistry and Biochemistry, Feodor-Lynen-Strasse 25, 81377 Munich, Germany.

†To whom correspondence should be addressed. E-mail: beckmann@lmb.uni-muenchen.de

specific and high-affinity binding of SRP and both subunits of SR to RNCs with a near one-to-one-to-one stoichiometry (Fig. 1). No substantial SRP-SR interaction was observed in the absence of either GTP or GMP-PNP (β, γ-imidoguanosine 5′-triphosphate), as expected.

The cryo–electron microscopy (cryo-EM) map shows the 80*S* ribosome at 7.4 Å resolution (fig. S1), with additional density stretching from the peptide exit site to the intersubunit space (Fig. 1). A difference in the domain appearance between Alu and S domains of SRP (*14*) probably reflects the higher flexibility of the S domain in the newly formed complex after SR interaction. Consequently, the α-helical secondary structure of proteins is well resolved in the ribosome and the SRP Alu domain but not in density corresponding to the SR and S domain of SRP.

The Alu domain is rigidly bound to the ribosome in the exact same position in both the SRP-RNC complex (*14*) and the SR-SRP-RNC complex. Thus, the elongation retardation induced by the Alu domain (*19*) appears to persist during the docking phase and may be released only after successful transfer of the RNC to the translocon.

A clear difference between this reconstruction and the structure of the SRP-RNC complex (*14*) is the additional density visible on the S domain of SRP near the previously described connection C4. In difference calculations, a strong signal appeared in this region and can, thus, be assigned to additional density provided by SR (Fig. 2A). It contacts both the S domain of SRP and the 60*S* ribosomal subunit, confirming a "dual" binding mode of SR to both SRP and the ribosome (*6*). This density corresponds very well to the structure of the mammalian SRαX1-SRβ heterodimer (*12*), for which two alternative orientations related by a 180° rotation are possible. The best-fitting model (correlation coefficient of 0.82 versus 0.78) positions the SRαX1-SRβ heterodimer such that the SRβ subunit interacts with 7*S* RNA of SRP and also with two ribosomal components, protein L31 and helix 99 of 25*S* ribosomal RNA (rRNA) (Fig. 2, B and C). This is in agreement with cross-linking data showing a ribosomal protein of 21 kD (possibly representing L31) in the immediate vicinity of SRβ (*18*). The linker between the globular domain of the SRβ subunit and the transmembrane helix comprises seven amino acids and is long enough to span a maximum distance of about 25 Å between the observed position of SRβ and the membrane. In this position, the SRαX1 domain interacts only with the 7*S* RNA of SRP and the SRP68/72 protein heterodimer and is close to but does not participate directly in the interaction with the ribosome, as suggested (*6*). Involvement of the SRP68/72 heterodimer may explain the observation that alkylation of SRP68/72 yields

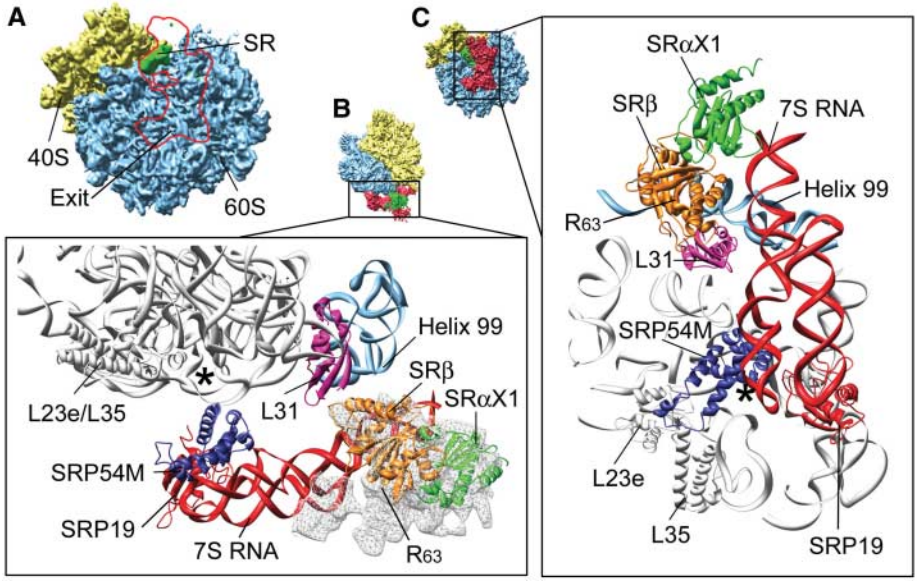

Fig. 2. Difference map and docking of the SRαX1-SRβ heterodimer. (**A**) Bottom view of the EM map of the RNC-SRP-SR complex together with the difference map (green, SR) indicating additional density as compared with the RNC-SRP map. The contour of the SRP S domain/SR density is shown as a red line. (**B**) Molecular models docked into the EM densities (side view). White mesh, extra density in the RNC-SRP-SR complex; green and orange, mammalian SRαX1-SRβ heterodimer; white ribbons, 25*S* rRNA and proteins L23e/L35; bright blue, helix 99 of 25*S* rRNA; pink, ribosomal protein L31; red ribbons, RNA of SRP S domain and SRP19 protein; dark blue, SRP54M domain. R63 indicates the N-terminal Arg^{63} of the reconstituted SRβ construct, in the wild-type protein, connecting with the transmembrane domain. Asterisk indicates the tunnel exit. (**C**) Same as (B) but oriented as in (A).

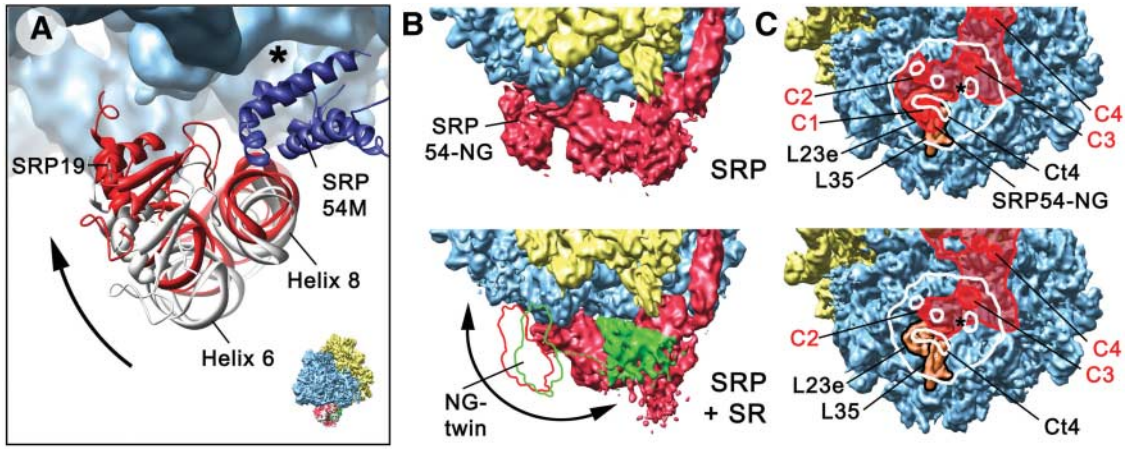

Fig. 3. Rearrangement of SRP S domain and exposure of translocon binding site. (**A**) The 60*S* subunit is shown together with molecular models for the SRP S-domain RNA and SRP19 in the absence (white) or presence of SR (red). The arrow indicates the rotation toward the ribosome. The SRP54 M domain is shown in dark blue, and the inset indicates the orientation. (**B**) Comparison of the RNC-SRP (top) and the RNC-SRP-SR (bottom) reconstructions, with color code as in Fig. 1. The position of the SRP54 NG domain (top) and of the expected position of the SRP/SR NG twin (bottom, red and green contour) is indicated. The arrow indicates the possible movements of the delocalized NG twin and the dashed green line the linker (SRαX2) between the SR NG domain and SRαX1. (**C**) The map of the ribosome is shown together with the SRP S domain (transparent red area with red contour) in the absence (top) and presence of SR (bottom). L23e and L35 are shown in orange. C1 to C4 (red) point to the connections between SRP and the ribosome. The translocon and its ribosomal connections are indicated by a white contour; Ct4 points to the main connection described previously (*15*). The ribosomal tunnel exit is indicated by an asterisk in (A) and (C). The L23e/L35 adaptor site is exposed in the presence of SR.

a particle that no longer interacts functionally with SR (*20*). Additional density indicates that the positively charged SRαX2 linker domain stretches from the position of the SRαX1-SRβ heterodimer parallel along the SRP RNA toward the M domain.

To address the possibility that the targeting complex serves as a GAP for SRβ (*21*), resulting in dissociation of SRβ from SRα, we used a mutant SRβ containing a GTPase-inactivating point mutation H119A (replacement of His^{119} with Ala) (*22*). However, the absence of major differences between the mutant cryo-EM structure (at 9 Å) (fig. S2) and the wild type suggests that no substantial GTP hydrolysis by SRβ and no SR dissociation take place under the conditions in our study. This indicates that the SRP-RNC complex is not sufficient to act as a GAP for SRβ (*6*).

Another difference between the SR-SRP-RNC structure and the SRP-RNC complex (*14*) is the overall behavior and position of the SRP S domain. It is not as rigidly bound to the ribosome as it is without SR, and it rearranges with respect to the 60*S* ribosomal subunit by a rotation of ~10° toward the ribosome (Fig. 3A). The axis of the rotation runs from SRP connection C4 to connections C2/C3 parallel to helix 8 of SRP RNA. As a result, the S domain moves away from the peptide exit site and, at the same time, closer to the ribosome (Fig. 3A). No rearrangements beyond connection C4 toward the Alu domain of SRP could be identified, which implies that within the observed limits the conformations of Alu and S domain can be uncoupled due to the flexibility of hinge 1 (*14*).

The third and most prominent difference between the docking and the targeting complex is the apparent delocalization of both NG domains and loss of connection C1 (Fig. 3B). As one possibility, we expected to recognize a twin-like arrangement, as observed in the complex formed by the isolated NG domains of bacterial SRP and SR (*9*, *10*). However, although the SR binding is GTP dependent and SRα and SRP54 can be detected as full-length proteins in the reconstitution assay (Fig. 1A), density for the two NG domains is completely absent. Thus, the suggested interaction of the two NG domains is likely to lead to delocalization of the flexible SRP54 NG domain (*23*), possibly due to rearrangement of the ribosome-interacting N domain of SRP54 as observed in isolated NG heterodimer structures (*9*, *10*). As a result, SRP breaks its connection with the ribosome (C1), and a site composed of the ribosomal proteins L23e and L35 (L23p and L29p in *E. coli*) is exposed (Fig. 3, B and C). This is in agreement with the cross-link pattern between SRP54 and L23e/L35, which changes in response to SR interaction (*16*). Moreover, several lines of biochemical evidence also point to a conformational change of SRP54 upon SR interaction, and distinct conformations of the SRP-SR complex have been suggested (*24*–*26*). However, the results are not directly comparable.

The SRP binding site (C1) cleared by the NG delocalization is the universal ribosomal adaptor site used by many factors that interact with the emerging nascent chain (*14*–*16*, *27*, *28*). In particular, the two ribosomal proteins L23e and L35 provide a major binding site (Ct4) for the translocon in eukaryotes (*15*) and also in prokaryotes (*29*). Although additional translocon binding sites (*15*, *29*) are still covered, exposure of this site thus allows initial spatial access of the translocon (Fig. 3C). When interacting with this site, the translocon would not only be close to the ribosomal tunnel exit, but it would also be in the immediate vicinity of the signal sequence–binding M domain of SRP54, a position suitable for direct transfer of the signal sequence from SRP.

Taken together, our results explain how SR interacts with both the ribosome and SRP, rendering the targeted RNC competent to interact with the translocon and primed for transfer of the signal sequence (Fig. 4): The Alu domain of SRP stays firmly bound to the ribosome to maintain elongation arrest, whereas the entire S domain is destabilized. Most important, after interaction of the NG domains, a major translocon binding site is exposed by a conformational change that results in the SRP54 NG domain being disconnected from the universal adaptor site. It remains to be shown how the presence of a translocon coordinates subsequent signal sequence transfer and triggers GTP hydrolysis by the SRP system (*4*) and subsequent SRP-SR dissociation.

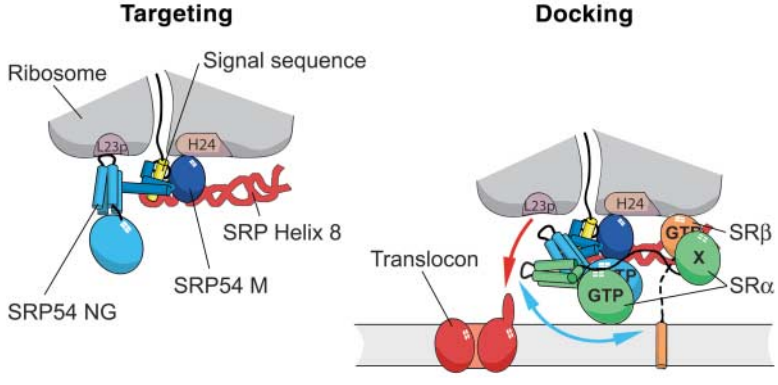

Fig. 4. Dynamic behavior of SRP upon SR interaction. SR interaction with RNC and SRP induces rearrangement of the S domain but leaves the Alu domain unchanged: The NG domain of SRP54 is delocalized after NG-twin formation (cyan arrow), resulting in exposure of the L23e/L35 universal ribosomal adaptor site and access of the translocon to its ribosomal binding site Ct4 (red arrow).

References and Notes

1. R. J. Keenan, D. M. Freymann, R. M. Stroud, P. Walter, *Annu. Rev. Biochem.* **70**, 755 (2001).
2. M. Halic, R. Beckmann, *Curr. Opin. Struct. Biol.* **15**, 116 (2005).
3. P. J. Rapiejko, R. Gilmore, *Cell* **89**, 703 (1997).
4. W. Song, D. Raden, E. C. Mandon, R. Gilmore, *Cell* **100**, 333 (2000).
5. S. Angelini, S. Deitermann, H. G. Koch, *EMBO Rep.* **6**, 476 (2005).
6. E. C. Mandon, Y. Jiang, R. Gilmore, *J. Cell Biol.* **162**, 575 (2003).
7. A. A. Herskovits, E. Shimoni, A. Minsky, E. Bibi, *J. Cell Biol.* **159**, 403 (2002).
8. T. Schwartz, G. Blobel, *Cell* **112**, 793 (2003).
9. P. F. Egea *et al.*, *Nature* **427**, 215 (2004).
10. P. J. Focia, I. V. Shepotinovskaya, J. A. Seidler, D. M. Freymann, *Science* **303**, 373 (2004).
11. T. Powers, P. Walter, *Science* **269**, 1422 (1995).
12. O. Schlenker, A. Hendricks, I. Sinning, K. Wild, *J. Biol. Chem.* **281**, 8898 (2006).
13. I. Moller *et al.*, *Proc. Natl. Acad. Sci. U.S.A.* **95**, 13425 (1998).
14. M. Halic *et al.*, *Nature* **427**, 808 (2004).
15. R. Beckmann *et al.*, *Cell* **107**, 361 (2001).
16. M. R. Pool, J. Stumm, T. A. Fulga, I. Sinning, B. Dobberstein, *Science* **297**, 1345 (2002).
17. Materials and methods are available as supporting material on *Science* Online.
18. T. A. Fulga, I. Sinning, B. Dobberstein, M. R. Pool, *EMBO J.* **20**, 2338 (2001).
19. V. Siegel, P. Walter, *Nature* **320**, 81 (1986).
20. V. Siegel, P. Walter, *Cell* **52**, 39 (1988).
21. G. Bacher, M. Pool, B. Dobberstein, *J. Cell Biol.* **146**, 723 (1999).
22. K. R. Legate, D. Falcone, D. W. Andrews, *J. Biol. Chem.* **275**, 27439 (2000).
23. K. Wild, M. Halic, I. Sinning, R. Beckmann, *Nat. Struct. Mol. Biol.* **11**, 1049 (2004).
24. I. Buskiewicz, A. Kubarenko, F. Peske, M. V. Rodnina, W. Wintermeyer, *RNA* **11**, 947 (2005).
25. F. Chu *et al.*, *Proc. Natl. Acad. Sci. U.S.A.* **101**, 16454 (2004).
26. R. J. Spanggord, F. Siu, A. Ke, J. A. Doudna, *Nat. Struct. Mol. Biol.* **12**, 1116 (2005).
27. S. Q. Gu, F. Peske, H. J. Wieden, M. V. Rodnina, W. Wintermeyer, *RNA* **9**, 566 (2003).
28. I. Buskiewicz *et al.*, *Proc. Natl. Acad. Sci. U.S.A.* **101**, 7902 (2004).
29. K. Mitra *et al.*, *Nature* **438**, 318 (2005).

30. We thank G. Bozkurt for preparation of the mutant SR (SRβ H119A). This work was supported by grants from the VolkswagenStiftung (R.B.) and the Deutsche Forschungsgemeinschaft SFB449 (R.B.) and SFB638 (I.S.); by the Royal Society (M.R.P.); and by the European Union and Senatsverwaltung für Wissenschaft, Forschung und Kultur Berlin (UltraStructureNetwork). Coordinates have been deposited in the RCSB (Research Collaboratory for Structural Bioinformatics) Protein Data Bank with accession number 2GO5. The cryo–EM map has been deposited at the 3D-EM database (European Molecular Biology Laboratory–European Bioinformatics Institute, Cambridge, UK) with accession number EMD-1217.

Supporting Online Material

www.sciencemag.org/cgi/content/full/312/5774/745/DC1
Materials and Methods
Figs. S1 and S2
References

11 January 2006; accepted 3 April 2006
10.1126/science.1124864